RESEARCH | Article in Press

# Amygdala shows heterogeneous atrophy and tauopathy patterns across the AD continuum

**Yasmine Salman · Thomas Gérard · Lara Huyghe · Lise Colmant · Vincent Malotaux · Jean-Louis Bayart · Emilien Boyer · Flo Blondiaux Pirson · Pascal Kienlen-Campard · Laurence Dricot · Renaud Lhommel · Adrian Ivanoiu · Lisa Quenon · Bernard J. Hanseeuw**

Received: 5 March 2026 / Accepted: 27 August 2026


## Abstract

**Background** Amygdala shows early vulnerability in Alzheimer's disease (AD), although its substructures have been less studied than hippocampal subfields. Neuropathological evidence suggests that tau pathology affects amygdala subnuclei differentially, yet in vivo characterization of subregional amygdala atrophy, its relationship with tau burden, blood-based biomarkers, and cognitive outcomes across the AD continuum remains limited. Clarifying whether amygdala degeneration follows a homogeneous or regionally selective pattern, how it relates to plasma tau biomarkers, and whether it has functional consequences is essential for improving early detection and disease modeling.

**Methods** The study analyzed data from 197 participants, including 71 Aβ-negative cognitively normal individuals (Aβ− CN), 31 Aβ-positive cognitively normal individuals (Aβ+ CN), and 95 Aβ-positive cognitively impaired individuals (Aβ+ CI). All participants underwent T1-weighted MRI, [$^{18}$F]-MK-6240 tau PET imaging, comprehensive neuropsychological assessment, and plasma pTau181 and pTau217 and Aβ42/40 analyses. Amygdala subregion volumes and tau standardized uptake value ratios (SUVr) were extracted using FreeSurfer-based segmentation and classified into basal, centro-medial, and lateral amygdala subregions. Regional amygdala volumes and SUVr were compared across groups and examined for associations with plasma tau biomarkers and cognitive performance. Mediation analyses assessed whether subregional amygdala atrophy mediated the relationship between tau pathology and cognition.

**Results** Pronounced regional heterogeneity was observed within the amygdala. Atrophy of the centro-medial subregion was detectable at the preclinical stage of AD, preceding cognitive impairment. Lower centro-medial amygdala volume was significantly associated with higher plasma pTau181 and pTau217 levels, as well as with lower memory and executive scores. Mediation analyses demonstrated that amygdala tau-PET burden fully mediated the relationship between plasma pTau biomarkers and centro-medial amygdala volume, while centro-medial amygdala volume mediated the effect of tau pathology on memory performance. Although the centro-medial subregion showed the earliest and most pronounced atrophy, it did not exhibit a correspondingly higher local tau-PET burden than other amygdala subregions.




https://doi.org/10.1186/s13195-026-02172-8

Published online: 05 September 2026

**Conclusion** These findings suggest that amygdala involvement in AD is regionally heterogeneous, appears early in the AD continuum, and has clinically significant cognitive consequences. Subregional quantification of the amygdala, particularly when combined with plasma pTau biomarkers, may provide sensitive early indicators of disease-related neurodegeneration, reflect network-level vulnerability, and improve understanding of cognitive decline, confirming its potential utility as a biomarker in AD research and clinical practice.

**Abbreviations**

| | |
|---|---|
| Aβ | Amyloid-beta |
| AD | Alzheimer's disease |
| APOE | Apolipoprotein E |
| CI | Cognitively impaired |
| CN | Cognitively normal |
| CSF | Cerebrospinal fluid |
| FOV | Field of view |
| MCI | Mild cognitive impairment |
| MMSE | Mini-Mental State Examination |
| MRI | Magnetic resonance imaging |
| MTL | Medial temporal lobe |
| NFTs | Neurofibrillary tangles |
| PET | Positron emission tomography |
| pTau | Phosphorylated tau |
| pTau181 | Phosphorylated tau at threonine 181 |
| pTau217 | Phosphorylated tau at threonine 217 |
| ROI | Region of interest |
| SD | Standard deviation |
| SUVr | Standardized uptake value ratio |
| TE | Echo time |
| TR | Repetition time |

## Background

Alzheimer's disease (AD) is characterized by progressive cognitive decline and the accumulation of amyloid-beta (Aβ) plaques and neurofibrillary tau tangles (NFTs) [1]. Among these pathological hallmarks, tau tangles are particularly closely linked to brain atrophy [2] and subsequent cognitive decline [3–5]. NFTs initially accumulate in the medial temporal lobe (MTL), including the transentorhinal cortex, entorhinal cortex, hippocampus, and amygdala, making this region critical in the early stages of AD pathology [6, 7].

Despite the early involvement of the entire MTL, most research on early AD has focused on the hippocampus (including hippocampal subfields) and the entorhinal and transentorhinal cortices [5, 8–13]. This focus is likely driven by their essential role in memory, the first cognitive domain affected in typical AD [1]. In contrast, the amygdala has been relatively understudied, despite being affected early in the disease process [14]. Studies have shown that the amygdala accumulates tau pathology early in AD [6, 15–20], at a similar stage to the hippocampus and entorhinal cortex [6, 14]. Atrophy of the amygdala has also been reported in preclinical AD stages [21–23]. Importantly, this atrophy appears to be heterogeneous across its subregions [21, 22], with the centro-medial nuclei potentially atrophying earlier [22]. Postmortem studies indicate that tau deposition also preferentially targets centro-medial amygdala [21, 24–27], suggesting a biological basis for this nonuniform vulnerability.

These observations raise the question of whether amygdala atrophy and tau pathology in AD are homogeneous across subnuclei or show regional heterogeneity, which can now be investigated in vivo using volumetric MRI and tau PET imaging [28, 29].

Besides imaging, recent advances in blood-based biomarkers allow very early detection of AD-related tau pathology, even before symptom onset [30, 31], and may help predict regional vulnerability within the amygdala. While pTau181 and pTau217 robustly relate to hippocampal volume and hippocampal atrophy over time [30, 32–34], only a few studies have investigated their associations with hippocampal subfield volumes [35, 36]. Investigation of subregion-specific amygdala atrophy has been even more limited, and whether plasma biomarkers can predict subregion-specific amygdala atrophy remains largely unknown.

Finally, although amygdala atrophy and amygdala tau pathology have been associated with memory performance and global cognitive decline [21, 29, 37–42], few studies have specifically examined the contributions of individual subregions to cognitive outcomes [29]. Thus, it remains unclear how early, subregion-specific atrophy may relate to functional deficits in AD.

These gaps lead to three key questions: (1) whether amygdala atrophy and tau pathology occur homogeneously or show regional heterogeneity across subnuclei in AD, (2) whether blood-based plasma biomarkers can predict subregion-specific amygdala atrophy, and (3) whether subregion-specific atrophy within the amygdala has measurable consequences for cognitive performance.

## Methods

### Participants

Non-demented older adults were enrolled in a study conducted at UCLouvain, Brussels, Belgium. Patients were recruited through the memory clinic of Cliniques Universitaires Saint-Luc, and volunteers were recruited from other studies via mailbox announcements in the hospital's neighborhood. Volunteers were selected from this pool to enrich the proportion of apolipoprotein E (APOE) ε4 carriers, thereby matching the observed frequency of APOE ε4 carriage in patients. Exclusion criteria for both patients and volunteers included focal brain lesions, epileptic seizures, major depression or other psychiatric disorders, and alcohol or drug abuse. Informed consent was obtained from all participants in accordance with the principles of the Declaration of Helsinki. Ethical approval for the study was granted by the UCLouvain Ethics Committee (13 May 2019; Eudra-CT number 2018-0034/73–94).

### Neuropsychological assessment

Each participant underwent a neuropsychological assessment evaluating four cognitive domains: memory, language, executive functions, and visuospatial functions. Memory was assessed with the Free and Cued Selective Reminding Test, French version [43]. Language was assessed with the Lexis Naming Test, the Category Fluency Test for animals, and the Letter Fluency Test for the letter "P" [44]. Executive functions were evaluated using the Trail Making Test and Luria's Graphic Sequences (French adaptations, unpublished), and visuospatial functions were assessed with the Clock Drawing Test and the Praxis subtest of the CERAD battery [45, 46]. Composite scores (*Z*-scores) were computed based on three measures for each cognitive domain, by referring to an independent sample of 32 Aβ- individuals who remained globally cognitively stable (as defined by a MMSE ≥ 26/30) over 8 years follow-up period (data collected in UCL-2010–412 study, see [47]).

A domain was considered impaired when the corresponding Z-score fell below −1.5 SD. Participants were classified as having cognitive impairment (CI) if they had least one impaired cognitive domain.

### Aβ status

Aβ status was determined by lumbar puncture or by Aβ-PET using either [$^{18}$F]Flutemetamol ($n$ = 85) or [$^{11}$C] Pittsburgh compound B ([$^{11}$C]PiB) ($n$ = 32). In cerebrospinal fluid (CSF), amyloid-β42 (Aβ42) and pTau181 were measured using Lumipulse automated assays ($n$ = 80). Aβ-PET quantification followed the Centiloid Aβ-PET [48], using the whole cerebellum as the reference region. Aβ status was considered positive if at least one of the following conditions was met: Centiloid > 21 or CSF Aβ42 < 437 pg/ml; or CSF Aβ42 < 650 pg/ml combined with CSF P-tau > 61 pg/ml [49, 50].

In total, 197 participants were included and categorized according to bioclinical classification based on Aβ status and neuropsychological evaluation: Aβ− CN ($n$ = 71), Aβ+ CN ($n$ = 31), and Aβ+ CI ($n$ = 95). Aβ− CN individuals who showed visually positive [$^{18}$F]MK-6240 Tau-PET exam were excluded from the analysis, as they do not cover the AD spectrum but might represent non-AD pathologies as Primary-Age Related Tauopathy ($n$ = 9) [51, 52]

### MRI

Three-dimensional T1-weighted MRI sequences were acquired on a 3 Tesla scanner (GE Signa Premier 3T, GE Healthcare, Chicago, IL) equipped with a 48-channel phased-array head coil. Two acquisition protocols were used, with the first applied to the initial 60 participants who underwent 3D T1 MRI as part of a European study that was not extended to the remainder of the present cohort.

For acquisition protocol 1, 196 slices were collected using the following parameters: repetition time (TR) = 7.2 ms, echo time (TE) = 2.9 ms, flip angle = 11°, slice thickness = 1.2 mm, field of view (FOV) = 270 × 270 mm$^2$, acquisition matrix = 256 × 256, and acquired voxel size = 1.05 × 1.05 × 1.2 mm$^3$.

For acquisition protocol 2, 156 slices were collected using the following parameters: TR = 2188 ms, TE = 2.9 ms, inversion time = 900 ms (MPRAGE), flip angle = 8°, slice thickness = 1 mm, FOV = 256 × 256 mm$^2$, acquisition matrix = 256 × 256, and acquired voxel size = 1 × 1 × 1 mm$^3$.

When available ($n$ = 177 of 197 participants), a 3D T2-weighted MRI scan was also acquired to improve the segmentation of amygdala subnuclei.

Subcortical segmentation and cortical parcellation of structural MRI data were performed using FreeSurfer v7.2 [53]. First, FreeSurfer standard recon-all steps were applied to the individual structural data of all participants. Detailed segmentation was then performed for the amygdala subnuclei. The amygdala was first divided into nine subnuclei, including the lateral nucleus, basal nucleus, accessory basal nucleus, medial nucleus, central nucleus, paralaminar nucleus, cortical nucleus, cortico-amygdaloid transition, and anterior amygdala area [28]. Smaller subnuclei were then grouped to form the centro-medial amygdala, including the cortical, central, medial, and accessory basal nuclei, following previous work showing that the volumes of these subnuclei were associated with tau-PET signal in the ADNI database (Fig. 1 [23]). This centro-medial subdivision corresponds to a previously described anatomo-functional grouping of the amygdala [54]. Importantly, it encompasses nuclei reported to show early tau deposition, as well as nuclei structurally connected to brain regions exhibiting early NFT accumulation [14]. All regions were averaged over the left and right hemispheres.

### [$^{18}$F]MK-6240 tau-PET

[$^{18}$F]MK-6240 (Lantheus Inc.) is an investigational second-generation tracer for imaging cerebral tau tangles. Radiosynthesis was performed at KU Leuven, and the radiotracer was delivered to our clinic within one hour. Ninety minutes after intravenous administration of [$^{18}$F]MK-6240 (target activity 185 ± 5 MBq), a 30-minute dynamic list-mode acquisition was performed on a Philips Vereos digital PET/CT scanner (Philips Healthcare). Images were reconstructed using the manufacturer's algorithm, which included attenuation, scatter, and decay

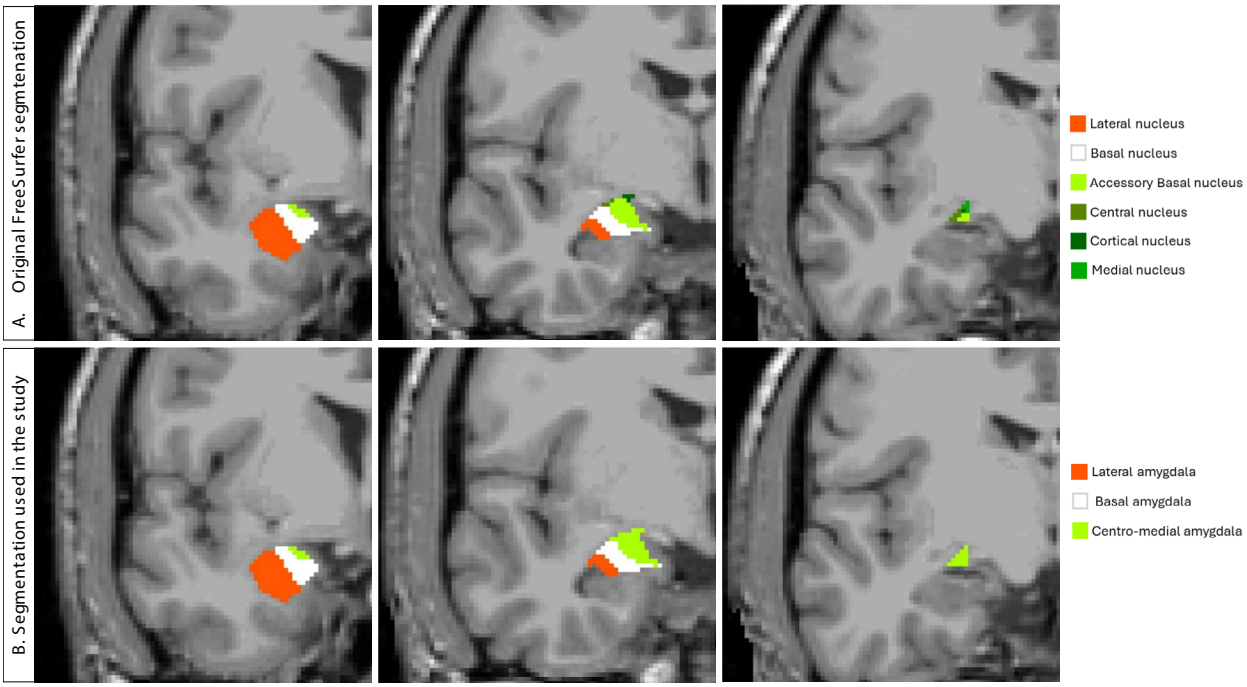


**Fig. 1** Illustration and comparison of amygdala segmentation. **A** Original segmentation provided by FreeSurfer. **B** Grouping of subnuclei used in the present study to form the centromedial amygdala

corrections as well as time-of-flight information. Point spread function (PSF) modeling and 1-mm reslicing were also applied to improve spatial resolution.

Tau-PET was co-registered with the corresponding T1-weighted MRI using the PetSurfer pipeline, a set of tools within FreeSurfer for end-to-end integrated MRI-PET analysis. A Geometric Transfer Matrix (GTM) partial volume correction was applied using PetSurfer before SUVr extraction. Standardized Uptake Value ratio (SUVr) values for the amygdala and amygdala subnuclei were extracted using cerebellum gray matter as a reference region**.** Amygdala SUVr was extracted using the Desikan-Killany atlas, while amygdala subnuclei SUVr values were recomputed manually. For each participant, the tau-PET image coregistered to the individual FreeSurfer amygdala subnuclei segmentation was loaded in MATLAB. The mean standardized uptake value (SUV) was extracted for each amygdala subnucleus and for the whole cerebellar cortex, which served as the reference region. The SUVr of each subnucleus was calculated as the mean SUV in the region of interest divided by the mean SUV of the cerebellar cortex. Left and right subnuclei were quantified separately and then combined into a weighted average based on the number of voxels to obtain a bilateral value. The overall SUVr of each of the centro-medial amygdala subnuclei was subsequently calculated as a weighted average of its subnuclei, with weights corresponding to the number of voxels in each subnucleus. Tau SUVr data were missing for 11 Aβ+ CI individuals, either because they missed the scanning session or due to acquisition-related issues. Of note, Aβ− CN showing tau pathology ($n$ = 9, all Braak-like stage ≤ 3) were not included in this study as they might represent primary age-related tauopathy (PART) [52, 55, 56].

## Blood-based biomarkers

Blood was collected in $K_2$-EDTA tubes, independently of fasting status, centrifuged at room temperature at 2500 g for 10 min, and plasma aliquots were frozen at −80°C within 2 hours. After 1 hour of thawing at room temperature, plasma pTau217 was measured with the Lumipulse® G pTau217 Plasma RUO assay (Fujirebio, Ghent,

Belgium) using Lumipulse analyzers (G600II). pTau181, Aβ42 and Aβ40 were measured on a Simoa® SR-X (pTau-181 V2.1; Neurology 3-Plex A).

pTau217 data were missing for 4 Aβ- CN, 1 Aβ+ CN and 31 Aβ+ CI individuals; pTau181 data were missing for 6 Aβ- CN, 7 Aβ+ CN and 32 Aβ+ CI individuals, while Aβ42/Aβ40 data were missing for 4 Aβ- CN, 2 Aβ+ CN and 31 Aβ+ CI individuals.

### Statistical analysis

First, demographic differences among the three groups (Aβ- CN, Aβ+ CN, Aβ+ CI) were assessed using Mann-Whitney tests for continuous variables and chi-square tests for categorical variables.

Next, group differences in amygdala subregion volumes and SUVr were assessed using linear regression models followed by post-hoc contrast analyses, adjusting for age, sex, intracranial volume, and, when appropriate, global amygdala volume or SUVr. Including global amygdala measures as a covariate determined whether observed differences were independent of overall amygdala effect. Then, to examine SUVr differences between subnuclei within each group, repeated measures ANOVAs were performed across regions. These analyses were conducted separately within each group to account for potential differences in overall tau distribution or atrophy patterns.

Subsequently, relationships between amygdala subregion volumes and SUVr with blood-based biomarkers were investigated using partial Spearman correlations, controlling for age, sex, intracranial volume, and global amygdala volume or SUVr. In parallel, the associations between amygdalar subnuclei volumes and cognitive z-scores were computed using partial Spearman correlations, adjusting for age, sex, years of education, and global amygdala volume.

Finally, to test whether the previously described association between tau pathology and cognition [3–5] was mediated by atrophy of the amygdalar subnuclei, a mediation analysis was conducted. This model evaluated whether the association between plasma biomarkers (p-tau181 or p-tau217) and cognitive outcomes (memory or executive composite scores) was mediated by variations in amygdala Tau-PET SUVr and centro-medial amygdala volume, while adjusting for age, sex, and education. All possible indirect pathways were tested. Total, direct, and indirect effects were estimated using a 5,000-iteration bootstrapping procedure [57].

All analyses were performed using R version 4.2.2 (packages *ppcor, emmeans, bda and lavaan*) and FDR-corrected for multiple comparisons.

## Results

### Demographics

The study included 197 participants, including 71 Aβ- cognitively normal (CN) individuals (36.4%), 31 Aβ+ CN individuals (15.7%), and 95 Aβ+ cognitively impaired (CI) individuals (48.2%). The groups did not differ in sex ($p = 0.59$) or intracranial volume ($p = 0.1$), but age differed significantly, with Aβ- CN participants being younger than both Aβ+ CN and Aβ+ CI participants ($p < 0.01$). APOE ε4 carrier status also differed between groups, with a significantly higher proportion of ε4 carriers in the Aβ+ CN and Aβ+ CI groups compared to the Aβ− CN group ($p < 0.05$). Level of education also differed, as Aβ+ CI participants had significantly fewer years of education compared to CN participants ($p < 0.01$).

Regarding global cognitive performance, Aβ− and Aβ+ CN individuals showed comparable Mini-Mental State Examination (MMSE) scores, which were significantly higher than those of Aβ+ CI participants ($p < 0.0001$). Across specific cognitive domains, Aβ+ CI participants exhibited lower memory, language, executive, and visuospatial composite scores compared to both Aβ− CN and Aβ+ CN individuals. In addition, Aβ+ CN participants showed lower executive functioning scores compared to Aβ− CN individuals ($p < 0.05$).

Aβ+ CI participants also had higher levels of tau biomarkers, including Amygdala SUVr, pTau217, and pTau181 than Aβ+ CN participants ($p < 0.0001$), who in turn had higher levels than Aβ- CN participants ($p < 0.0001$) (Table 1).

## Prominent atrophy of the centro-medial amygdala across the AD spectrum

We first aimed to investigate the heterogeneity of amygdala atrophy across the AD spectrum. Amygdala subnuclei volumes were compared between groups, adjusting for age, sex, and intracranial volume. We observed that the volume of the centro-medial amygdala subnuclei was significantly reduced in both CN Aβ+ ($\beta = 23.49$ mm$^3$, $p < 0.05$) and CI Aβ+ ($\beta = 62.24$ mm$^3$, $p < 0.0001$) groups compared to CN Aβ- individuals (Fig. 2). Basal and Lateral amygdala were only reduced in CI Aβ+ compared to CN Aβ- (Basal: $\beta_{basal} = 64.58$ mm$^3$, $p_{basal} < 0.0001$; Lateral: $\beta_{lateral} = 73.61$ mm$^3$, $p_{lateral} < 0.0001$; Fig. 2). Furthermore, after additionally controlling for global amygdala volume, the CI Aβ+ group still exhibited significantly lower centro-medial amygdala volume ($\beta = 13.85$ mm$^3$, $p < 0.01$), which was not the case for other amygdala subnuclei, indicating that centro-medial amygdala atrophy was more pronounced than global amygdala atrophy. Additional analyses accounting for education or APOE ε4 carrier status yielded similar results, indicating that the observed pattern of amygdala subregional atrophy was not driven by years of education or APOE genotype.

## Tau pathology does not preferentially deposit in the centro-medial amygdala

To investigate whether the centro-medial amygdala atrophy was explained by a heterogeneous distribution of tau pathology within the amygdala, we compared amygdala subnuclei SUVr between groups, adjusting for age and sex. SUVr in all amygdala subnuclei progressively increased at each stage of AD (CN Aβ+ and CI Aβ+; Fig. 3). When the model was adjusted for global amygdala SUVr, no group differences remained significant.

However, within-group comparisons of subnuclei SUVr across regions revealed that in both CN Aβ+ and CI Aβ+ groups, the Basal amygdala showed higher tau-PET signals than other subnuclei (CN Aβ+ : Lateral: $\beta_{lateral} = 0.32$, $p_{lateral} < 0.01$; centro-medial: $\beta_{centro\text{-}medial} = 0.6$, $p_{centro\text{-}medial} < 0.01$; CI Aβ+ : Lateral: $\beta_{lateral} = 0.84$, $p_{lateral} < 0.0001$; centro-medial: $\beta_{centro\text{-}medial} = 0.91$, $p_{centro\text{-}medial} < 0.0001$), and the global amygdala ($\beta = 0.6$, $p < 0.0001$; Fig. 3), suggesting a heterogeneous distribution of tau pathology within the amygdala, but not in the

**Table 1** Characteristics of the participants

| | Aβ- CN | Aβ+ CN | Aβ+ CI | Post-Hoc comparisons |
|---|---|---|---|---|
| N | 71 | 31 | 95 | |
| Age (years) | 67.52 ± 8.49 | 73.68 ± 5.86 | 71.22 ± 8.36 | Aβ- CN < Aβ+ CN ≈ Aβ+ CI |
| Sex (%F) | 59.16 | 51.61 | 51.58 | Aβ- CN ≈ Aβ+ CN ≈ Aβ+ CI |
| ApoE ε4 carrier (%) | 42.25 | 63.33 | 62.22 | Aβ- CN < Aβ+ CN ≈ Aβ+ CI |
| Education (years) | 16.89 ± 3.38 | 17.2 ± 3.38 | 14.92 ± 3.79 | Aβ- CN ≈ Aβ+ CN < Aβ+ CI |
| MMSE | 28.81 ± 1.03 | 28.67 ± 1.02 | 24.49 ± 3.63 | Aβ- CN ≈ Aβ+ CN < Aβ+ CI |
| Memory Z-score | 0.21 | 0.04 | −3.40 | Aβ- CN ≈ Aβ+ CN < Aβ+ CI |
| Langage Z-score | −0.07 | −0.01 | −1.42 | Aβ- CN ≈ Aβ+ CN < Aβ+ CI |
| Executive Z-score | 0.29 | 0.05 | −1.48 | Aβ- CN < Aβ+ CN < Aβ+ CI |
| Visuo-spatial Z-score | 0.13 | −0.10 | −1.54 | Aβ- CN ≈ Aβ+ CN < Aβ+ CI |
| Total intracranial volume (mm$^3$) | 1528643 ± 136167 | 1471849 ± 162530 | 1480840 ± 160699 | Aβ- CN ≈ Aβ+ CN ≈ Aβ+ CI |
| Amygdala Tau (SUVr) | 0.66 ± 0.1 | 1.67 ± 0.66 | 2.02 ± 0.85 | Aβ- CN < Aβ+ CN < Aβ+ CI |
| Plasma pTau217 (pg/mL) | 0.17 ± 0.26 | 0.31 ± 0.19 | 0.70 ± 0.47 | Aβ- CN < Aβ+ CN < Aβ+ CI |
| Plasma pTau181 (pg/mL) | 20.29 ± 9.59 | 31.44 ± 13.39 | 43.23 ± 23.70 | Aβ- CN < Aβ+ CN < Aβ+ CI |
| Plasma Ab42/40 | 0.049 ± 0.013 | 0.040 ± 0.009 | 0.041 ± 0.008 | Aβ- CN > Aβ+ CN ≈ Aβ+ CI |

Differences between groups were assessed with the Mann–Whitney or Fisher tests. Symbol meanings: "≈" indicates no statistically significant difference ($p > 0.05$); "<" indicates a statistically significant difference ($p < 0.05$), with the group on the left having lower values than the group on the right; ">" indicates a statistically significant difference ($p < 0.05$), with the group on the left having higher values than the group on the right

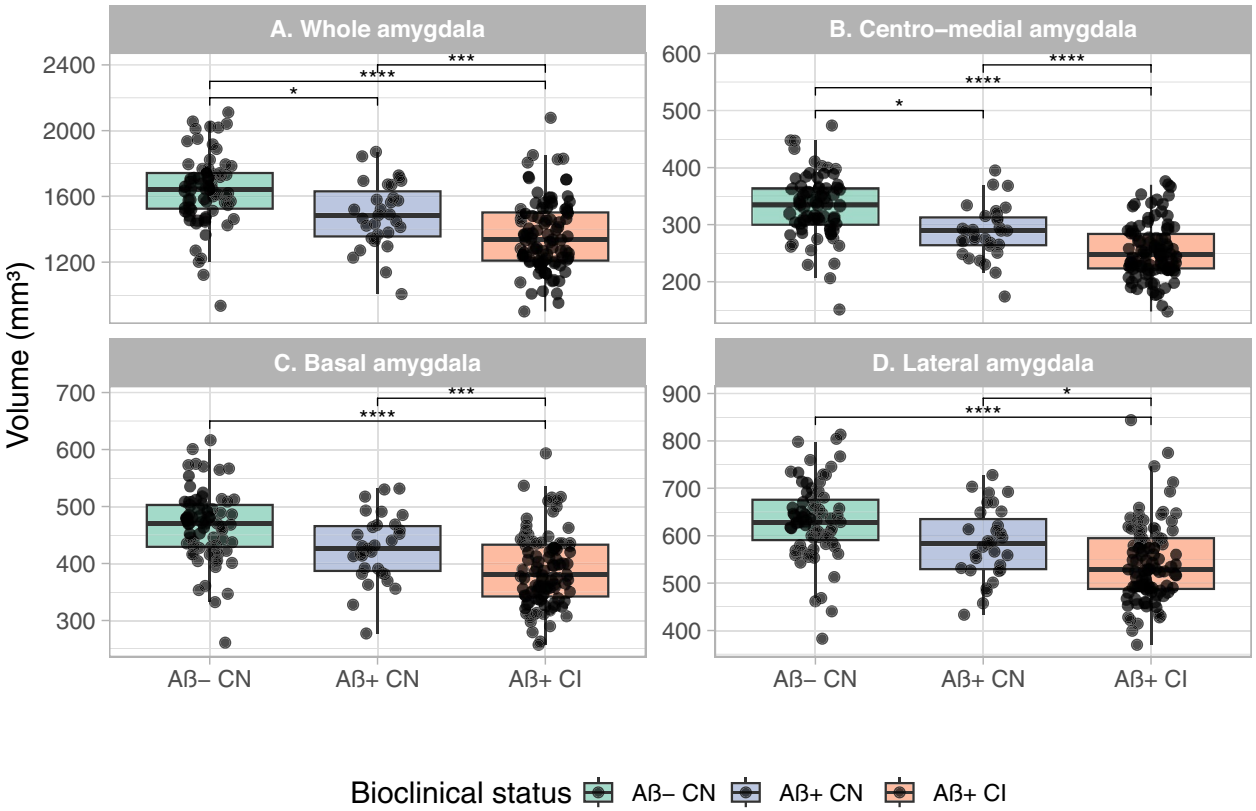


**Fig. 2** Amygdala volumes differences across bioclinical groups. Boxplots represent **A** global amygdala, **B** centro-medial amygdala, **C** basal amygdala, **D** lateral amygdala volumes per group. This analysis includes 197 participants, including 71 Aβ- CN (green), 31 Aβ+ CN (blue), and 95 Aβ+ CI (orange) individuals. Reported p-values are p-values adjusted for age, sex, and intracranial volume : *$p < 0.05$; **$p < 0.01$; ***$p < 0.001$; ****$p < 0.0001$. Sample size (N): Aβ- CN = 71, Aβ+ CN = 31, Aβ+ CI = 95

centro-medial amygdala, which was shown to be particularly atrophic compared with other amygdala subregions. This pattern remained largely unchanged after stratification by APOE ε4 carrier status.

## Blood pTau biomarkers predict centro-medial amygdala atrophy, which mediates episodic memory deficits

To examine the relationship between blood-based biomarkers and amygdala heterogeneity, we first investigated partial Spearman correlations between plasma biomarkers and amygdala subnuclei volumes. After adjusting for age, sex, education, and amygdala volume, only centro-medial amygdala volume was significantly associated with pTau measures ($R_{pTau217} = -0.21$, $p_{pTau217} < 0.01$; $R_{pTau181} = -0.22$, $p_{pTau181} < 0.01$, Fig. 4A left) but not with the plasma Aβ42/40 ratio (R = 0.10, p = 0.23; Fig. 4A left). In contrast, no blood-based biomarker correlated with amygdala subregion SUVr after adjusting for global amygdala SUVr (Fig. 4A left). In short, elevated pTau concentrations were associated with subregional amygdala atrophy, but not with subregional tau-PET measurements.

We then examined partial Spearman correlations between amygdala subregional volumes and cognitive performance ($N = 197$). We first examined correlations between amygdala subregion volumes and cognitive $Z$-scores, adjusting for age, sex, education, and amygdala volume. We observed that the centro-medial amygdala was associated with episodic memory ($R = 0.26$, $p < 0.05$) and executive (R = 0.21, $p < 0.05$) composite scores but not with visuospatial ($R = 0.16$, $p = 0.08$) or language scores ($R = 0.15$, $p = 0.09$; Fig. 4A right). In contrast, the volume of the other amygdala subregions was not associated with cognition after adjusting for global amygdala.

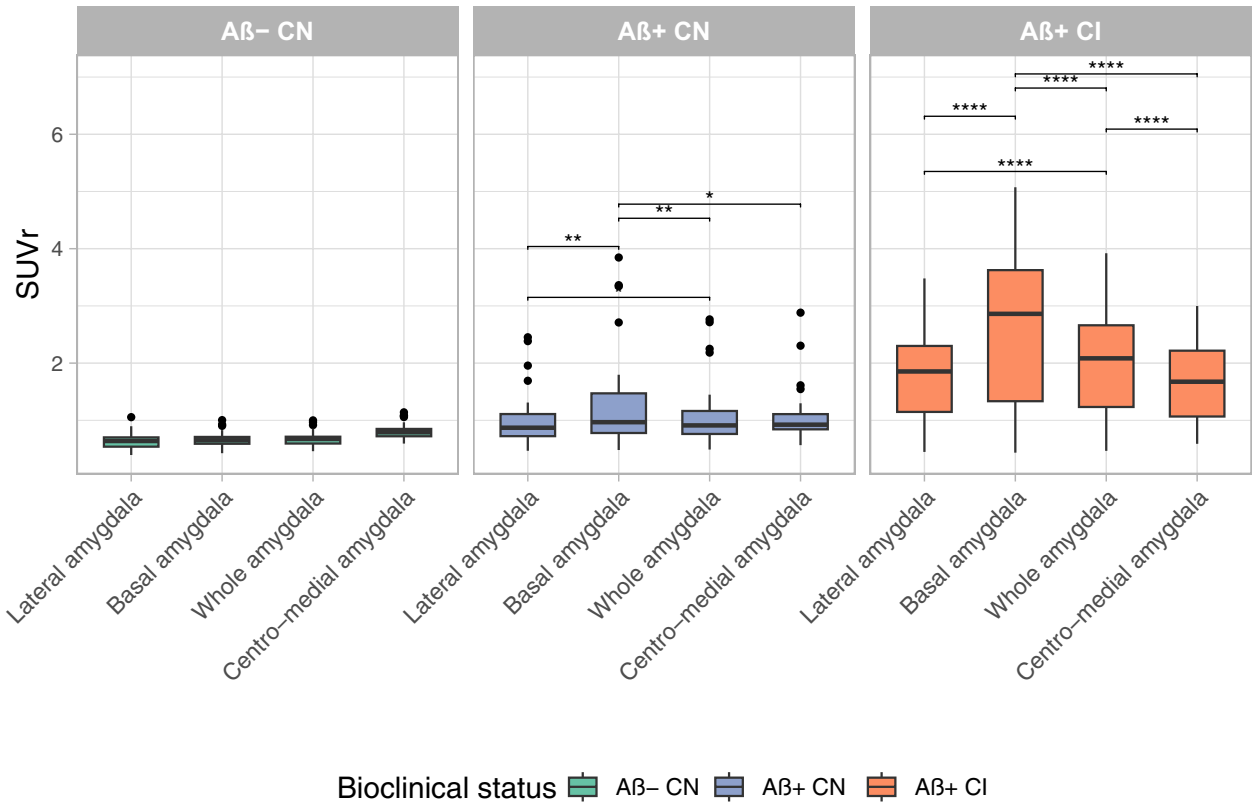


**Fig. 3** Tau-SUVr differences across amygdala subregions, stratified by bioclinical group. Boxplots show SUVr values for global, centro-medial, basal, and lateral amygdala for each group: 71 Aβ- CN (green), 31 Aβ+ CN (blue), and 84 Aβ+ CI (orange) individuals. Reported p-values correspond to comparisons across regions within each group, adjusted for age, sex, and intracranial volume: *$p < 0.05$; **$p < 0.01$; ***$p < 0.001$; ****$p < 0.0001$. Sample sizes correspond to participants with available tau-PET data and were : Aβ- CN = 71, Aβ+ CN = 31, Aβ+ CI = 84.

Similar results were observed when adjusting for global hippocampal volume/SUVr or entorhinal cortex volume/SUVr, which are involved in episodic memory (Supplementary Figures 1–2). Similarly, the associations between plasma pTau biomarkers and centro-medial amygdala volume remained significant after adjustment for APOE ε4 carrier status.

After highlighting the association of centro-medial amygdala volume with both plasma pTau and episodic memory performance, we aimed to test whether centro-medial amygdala volume could mediate the effect of tau pathology on cognition. Both plasma pTau and amygdala Tau-PET SUVr were included in the model, under the hypothesis that they may reflect distinct forms of tau pathology (circulating versus aggregated). To this end, a double mediation model was performed, assessing the relationships between plasma pTau (pTau181 or pTau217), amygdala Tau-PET SUVr, centro-medial amygdala volume, and memory composite scores (Fig. 5). The results showed that plasma pTau was associated with variations, first in amygdala Tau-PET SUVr ($\beta_{\text{pTau181 model}} = -0.48$; $\beta_{\text{pTau217 model}} = -0.53$; $p < 0.0001$), which in turn was associated with lower centro-medial amygdala volume ($\beta_{\text{pTau181 model}} = -0.41$; $\beta_{\text{pTau217 model}} = -0.38$; $p < 0.0001$). This sequence was finally associated with lower episodic memory performance (Indirect a*b $_{\text{pTau181 model}} = -0.05$; Indirect a*b $_{\text{pTau217 model}} = -0.06$; $p < 0.05$). After accounting for mediation, the direct association of pTau181 with memory composite score became nonsignificant, whereas the direct association of pTau217 remained significant, indicating only partial mediation by Tau-PET SUVr and centro-medial amygdala volume (Fig. 5). Notably, amygdala Tau-PET SUVr fully mediated the effect of plasma pTau on centro-medial amygdala volume (Indirect a*b $_{\text{pTau181 model}} = -0.24$; Indirect a*b $_{\text{pTau217 model}} = -0.26$; both p's < 0.0001). To evaluate whether clinical heterogeneity within the Aβ+ CI group influenced the

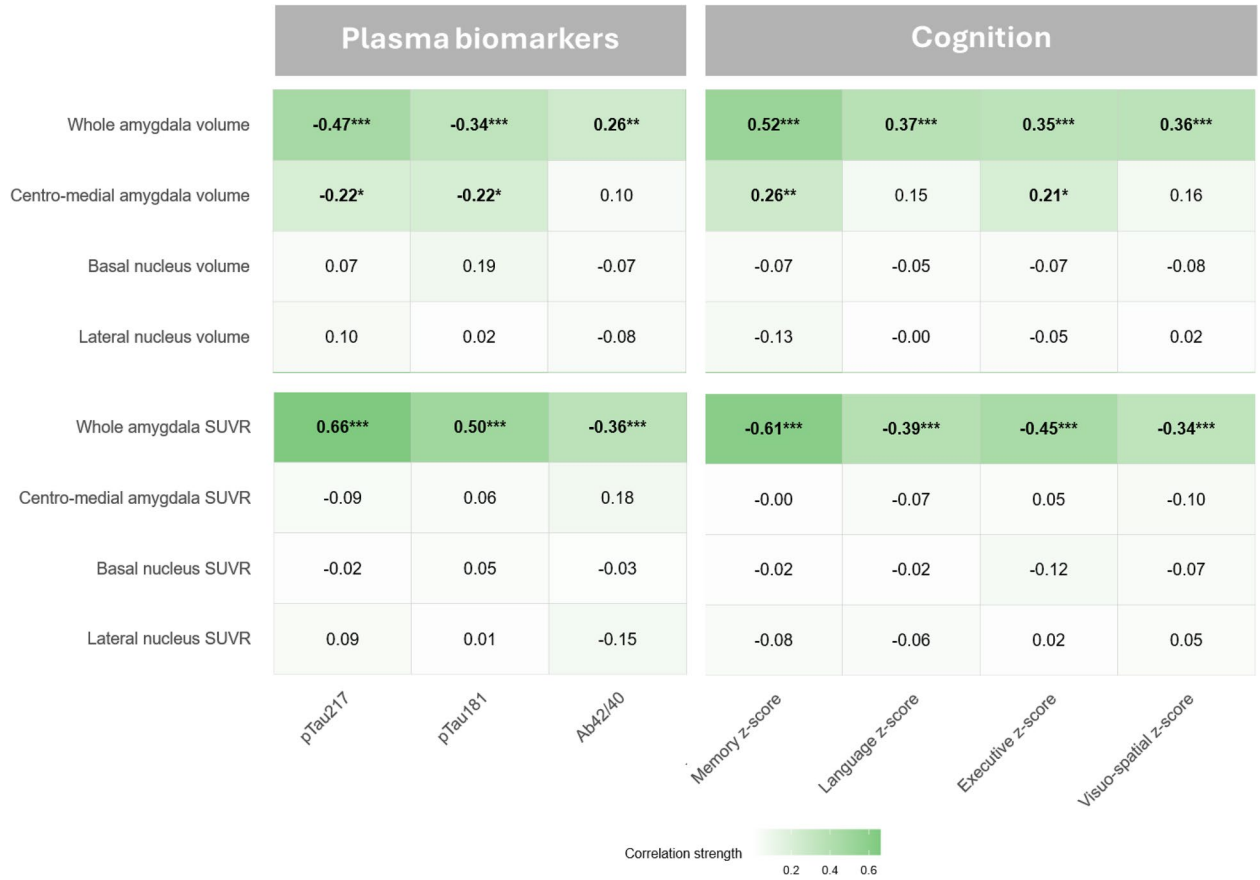


**Fig. 4** Relationships between amygdala subnuclei, SUVR, plasma biomarkers, and cognition. Heatmap of partial Spearman correlations between amygdala volumes or SUVr and blood-based biomarkers (pTau217, pTau181, Aβ42/40) and cognitive z-scores (Memory, Language, Executive, Visuo-spatial). Correlations were adjusted for age, sex, total intracranial volume, and global amygdala volume or SUVr; correlations involving cognition were additionally adjusted for education. Each cell shows the R value (green intensity = stronger correlation). Reported p-values: *$p < 0.05$; **$p < 0.01$; ***$p < 0.001$; ****$p < 0.0001$. Sample sizes varied according to data availability: pTau217, $n = 161$; pTau181, $n = 152$; Aβ42/40, $n = 160$; cognition and amygdala volumes, $n = 197$; cognition and tau-PET SUVr, $n = 186$. Differences in sample size reflect missing plasma biomarker and tau-PET data, as detailed in the Methods section.

mediation results, we performed sensitivity analyses restricted to CN or participants with memory impairment (memory composite z-score < −1.5 SD; N = 125). The mediation effect remained significant after excluding predominantly non-amnestic participants, yielding results that were highly consistent with the primary analysis (Supplementary Figure 3). Overall, these findings support the robustness of the main mediation results despite clinical heterogeneity within the Aβ+ CI group.

When the same model was applied to the executive composite score, the mediation was not significant (Indirect $a*b_{\text{pTau181 model}} = -0.04$, $p_{\text{pTau181 model}} = 0.14$; Indirect $a*b_{\text{pTau217 model}} = -0.04$; $p_{\text{pTau181 model}} = 0.17$; Supplementary Figure 4), suggesting that amygdala Tau-PET SUVr and centro-medial amygdala volume do not explain the effect of plasma pTau on executive dysfunction.

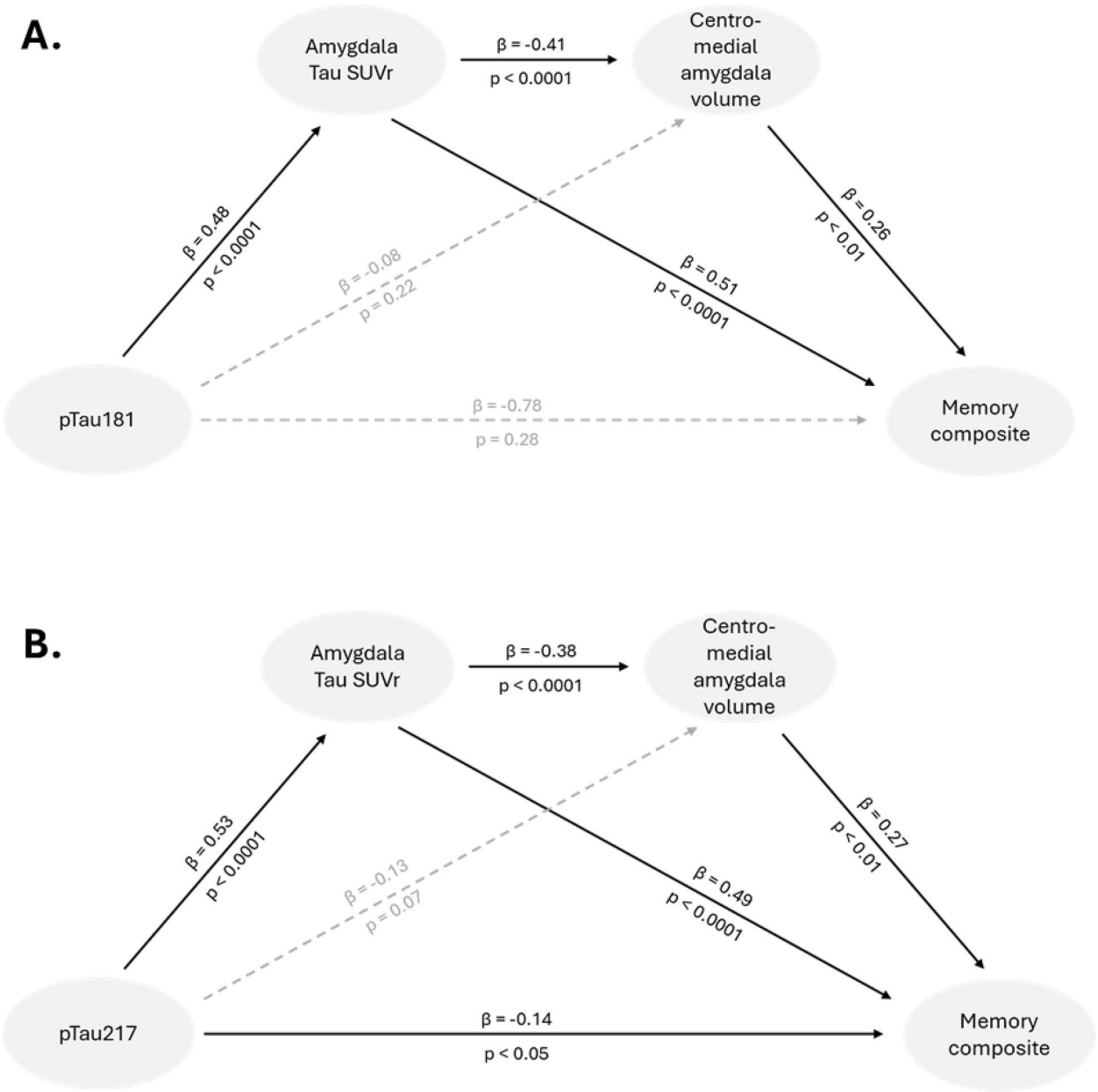


**Fig. 5** Mediation model pathways relating plasma pTau, amygdala tau SUVr, centromedial amygdala volume, and memory. Schematic representation of the mediation model examining the direct and indirect relationships among plasma pTau, amygdala tau SUVr, centromedial amygdala volume, and memory performance. Solid black lines indicate statistically significant pathways, whereas grey dotted lines represent alternative pathways that were not statistically significant. The model was adjusted for age, sex, and education. The sample size ($n$ = 152) corresponds to participants with complete data available for plasma pTau, amygdala tau-PET SUVr, centro-medial amygdala volume, and memory performance

## Discussion

In AD, amygdala exhibits early tau pathology and atrophy [6, 15–20, 22, 23] and is strongly associated with cognitive decline [3, 29, 38, 42, 58]. However, the amygdala is a heterogeneous structure composed of anatomically and functionally distinct subnuclei [40]. To determine whether these subnuclei are differentially affected across the AD continuum, we investigated amygdala heterogeneity in terms of atrophy and tau pathology, and their

relationships with cognition and blood-based biomarkers, in cognitively normal Aβ- individuals, preclinical AD, and symptomatic AD. We observed pronounced heterogeneity in amygdala atrophy, with earlier and more severe involvement of the centro-medial subregion compared with the basal and lateral nuclei. These findings align with prior neuropathological and post-mortem neuroimaging studies [19, 21, 24, 25, 59, 60]. They extend our previous findings of centro-medial amygdala atrophy in preclinical AD participants from ADNI [22] in a larger UCLouvain dataset with plasma, cognition, and amygdala subnuclei PET data.

In this current in vivo study, we aimed to examine whether the prominent atrophy of centro-medial amygdala reflects a non-uniform distribution of tau pathology within the amygdala. We did not observe a higher tau-PET signal in the centro-medial amygdala than in the basal nucleus in either preclinical or symptomatic AD. Interestingly, a recent study in familial AD also reported higher tau-PET signal in the basal nucleus [29]. Nevertheless, given the methodological limitations discussed below, convergence between studies should not be interpreted as definitive evidence regarding the true subnuclear distribution of tau pathology. In contrast, neuropathological investigations, including recent three-dimensional reconstructions, report greater tau deposition in the central, cortical, medial [24, 25, 59, 60] and accessory basal nuclei [19, 21], precisely corresponding to the centro-medial meta region-of-interest used in this work.

Several factors may contribute to this apparent discrepancy. First, the spatial resolution of PET (4x4x4 $mm^3$) may limit subnuclear quantification. This limitation is particularly relevant for the centro-medial amygdala because it is both smaller than the basal nucleus and more severely affected by atrophy across the AD continuum, resulting in only a limited number of PET voxels contributing to the signal within this subregion. Consequently, the centro-medial amygdala is more susceptible to partial volume effects, signal dilution, and spill-over effects, which may contribute to the apparently higher tracer uptake observed in the basal nucleus. Therefore, our findings should be interpreted with caution and do not allow definitive conclusions regarding the precise distribution of tau pathology across amygdala subnuclei. Second, off-target binding might account for higher tau-PET signal in the basal than in the centro-medial amygdala. However, basal amygdala tau-PET signal was low in Aβ-negative cognitively normal individuals, making this hypothesis less likely.

Another possible explanation may reside in regional differences in pathological deposition across amygdala subnuclei. Because amyloid deposition is thought to involve the amygdala relatively early in the disease process, consistent with Thal phase 2 [61], a substantial amyloid burden was likely already present throughout the amygdala in our Aβ+ participants. Such a pre-existing amyloid-rich environment may differentially influence vulnerability to tau accumulation and neurodegeneration across amygdala subnuclei. However, few studies have specifically investigated the regional distribution of amyloid pathology across amygdala nuclei and current neuropathological evidence does not fully support this idea. While Braak and Braak (1991) [6] described that "*the corticomedial complex of the amygdala reveals the presence of many neuritic plaques, while NFTs and neuropil threads predominate in the basolateral nuclei*", other studies have reported a greater density of senile plaques in basolateral nuclei, whereas neuronal loss and neurofibrillary tangles tend to predominate in corticomedial nuclei [24, 25, 60]. Finally, the apparent mismatch may not solely reflect interactions between amyloid and tau pathology. The amygdala represents a convergence hub for multiple neuropathological processes beyond amyloid and tau pathology, including TDP-43 pathology, α-synuclein pathology, vascular alterations, and other age-related proteinopathies [62]. Therefore, it cannot be excluded that additional neuropathologies not measured in the present study also contributed to the observed pattern of neurodegeneration across amygdala subnuclei. Future studies specifically investigating the spatial distribution of amyloid pathology across amygdala subnuclei, together with other co-pathologies, would therefore be valuable to clarify the respective contributions of amyloid pathology, tau aggregation, and neurodegeneration within the amygdala.

Building on these observations, the second aim of this study was to determine whether plasma biomarkers could capture the mechanisms underlying the selective vulnerability of the centro-medial amygdala. Plasma pTau181 and pTau217 concentrations, but not the Aβ42/40 ratio, were associated with reduced centro-medial amygdala volume. These results suggest that plasma pTau biomarkers relate to the biological processes underlying centro-medial amygdala degeneration. While current evidence indicates that plasma pTau181 and pTau217

primarily reflect amyloid-associated tau dysregulation [63], it has been hypothesized that these biomarkers may also capture a critical stage of disease progression during which tau pathology transitions from a soluble state toward aggregation and propagation within the brain [64], before becoming detectable with current in vivo tau-PET techniques [65]. Their association with centro-medial amygdala atrophy therefore suggests that plasma pTau biomarkers may reflect early tau-related pathological processes contributing to the selective vulnerability of this subregion.

Atrophy of the centro-medial amygdala was also related to cognitive deficits observed in AD. Specifically, centro-medial amygdala volume (but not the volumes of other amygdala subregions) was associated with both episodic memory and executive composite z-scores. This pattern supports a specific contribution of the centro-medial amygdala to cognitive performance and aligns with prior reports implicating the amygdala in episodic memory and executive processes [3, 29, 42]. The amygdala, particularly the medial nucleus, is also involved in affective symptoms such as depression and anxiety [66]. Although major depressive disorder was an exclusion criterion in the present study, minor depression is common in AD [67] and has been associated with tau pathology in the amygdala [29]. Such affective symptoms may therefore partly contribute to the observed associations between centro-medial amygdala volume and cognitive performance and cannot be fully excluded as a potential contributing factor.

Importantly, the centro-medial amygdala volume appeared to play a key intermediary role in the relationship between tau pathology and memory decline. The association between plasma pTau levels and memory performance was mediated by tau aggregation within the amygdala, as measured by amygdala tau PET SUVr, and by subsequent centro-medial amygdala atrophy. These findings are consistent with a hypothesized sequential relationship in which increased plasma pTau reflects early tau-related pathological processes, amygdala tau-PET signal reflects subsequent tau aggregation detectable in vivo, and centro-medial amygdala atrophy is associated with cognitive decline [68, 69]. However, given the cross-sectional nature of the present study, the temporal ordering of these events cannot be established directly and will require confirmation in longitudinal studies.

While the relationship between pTau181 and memory performance was fully mediated by amygdala tau PET uptake and centro-medial amygdala volume, the association involving pTau217 was only partially mediated. This suggests that pTau217 may capture additional pathological processes not fully reflected by amygdala tau PET imaging.

While previous studies have linked amygdala alterations to memory performance, our findings indicate that these associations may be driven specifically by the centro-medial subregion, potentially through its strong anatomical and functional connections with the entorhinal cortex and hippocampus [70, 71]. This selective vulnerability likely reflects a combination of local neuronal properties and network-level features, including connectivity patterns. By contrast, although prior studies have reported associations between the amygdala and executive functions, our findings indicate that the effect of tau pathology on executive performance is not mediated by amygdala involvement, either in terms of tau burden or volume loss. This observation is consistent with the predominant role of other brain regions, e.g., prefrontal cortical networks, rather than the amygdala or the medial temporal lobe in executive functioning [72].

Taken together, these results suggest that combining plasma pTau biomarkers with MRI-derived measures of centro-medial amygdala atrophy may provide an accessible early-warning signal for preclinical AD, limiting the need for PET imaging to the most at-risk CN older adults.

## Limitations and future perspectives

Technical limitations include automated segmentation at 1 $mm^3$ MRI resolution, co-registered with PET images at 4x4x4 $mm^3$, precluding direct visualization of amygdala subnuclei using PET. Although point spread function modeling and GTM partial volume correction were applied during PET processing, the spatial resolution of tau PET remains limited relative to the size of amygdala subnuclei. Consequently, residual partial volume effects may still influence subnuclear SUVr estimates and restrict our ability to draw definitive conclusions regarding the

precise distribution of tau pathology across amygdala subregions. Future studies using ultra-high-field MRI (7T or above) or novel PET instruments providing higher spatial resolution could refine subnuclear volumetry and validate segmentation algorithms.

Other methodological limitations included that individual amygdala subnuclei cannot be directly visualized on conventional in vivo MRI, subnuclear segmentation could not be manually verified, and relies entirely on the anatomical priors incorporated within the FreeSurfer segmentation algorithm.

Additionally, our cohort is not representative of the general population. It was enriched in APOE ε4 carriers among cognitively normal participants, which may limit the generalizability of the findings. Moreover, the sample predominantly consisted of highly educated White/Caucasian individuals, further restricting the extent to which these results can be extrapolated to more diverse populations.

Additional limitations include the lack of neuropsychiatric (including depression and anxiety) and olfactory assessments; given the amygdala's role in emotion and olfaction [14, 71], it would be valuable to determine whether centro-medial atrophy predicts early behavioral or sensory deficits. Future studies should also consider the amygdala within its functional networks to improve our understanding of how tau pathology and atrophy spread within the medial temporal lobe in AD.

Importantly, longitudinal studies are needed to determine whether trajectories of centro-medial versus basal/lateral amygdala atrophy can predict clinical progression from preclinical AD to MCI and from MCI to AD dementia [21]. Longitudinal studies will also be required to determine whether the temporal ordering suggested by our mediation analyses - linking plasma pTau, amygdala tau burden, centro-medial amygdala atrophy, and memory decline - reflects the true sequence of pathological events in AD.

## Conclusion

Overall, our results demonstrate that amygdala involvement in AD is heterogeneous, detectable from the preclinical stage, and has a clinical impact on cognition. Subregional amygdala quantification, particularly when combined with plasma pTau biomarkers, may provide early-warning signals of disease, highlight network-level vulnerability, and improve predictive models of progression, supporting its potential as a biomarker in AD research and clinical practice.

**Supplementary Information** The online version contains supplementary material available at https://doi.org/10.1186/s13195-026-02172-8.

**Acknowledgements** Y.S. is a FRIA grantee of the Fonds de la Recherche Scientifique – FNRS (FRIA40014635). L.H. is a research fellow of the Fonds de la Recherche Scientifique – FNRS (FNRS40016560). V.M. was funded by Wallonia-Brussels International (WBI World Fellowship). L.Q. is a postdoctoral research fellow of the Fonds de la Recherche Scientifique – FNRS (FC 95854). B.H. was funded by the FNRS, grant number CCL40010417, the FRFS-WELBIO, grant number 40010035, and Fondation Recherche Alzheimer/Stichting Alzheimer Onderzoek, grant numbers SAO20210026 and SAO20240044. We also thank the Fondation Louvain and the Saint-Luc Foundation for providing in-kind contributions.
The authors thank Marine Van Calsteren, lab technician, for the processing of plasma data; Daniela Savina and Fiona Galande, research coordinators, for recruitment and study coordination; and Julia Goloubeva and Camille Valenza, master's students at the time of data collection, for their assistance with MRI data acquisition as well as Paul Dulieu, master's student at the time of data collection, for his assistance with neuropsychological data collection.

**Authors' contributions** **YS** contributed to the study conception and design, MRI data collection and processing, PET data processing, formal statistical analysis, and drafted the first version of the manuscript. **LC** and **VM** contributed to MRI data collection and processing. **LC** also contributed to PET data processing and to the development of analysis scripts for MRI/PET analyses. **TG** and **RL** contributed to PET-tau data collection and processing. **LH** and **LQ** contributed to neuropsychological data collection and processing and provided feedback on cognition analysis. **JLB** and **EB** contributed to method development and to the collection and processing of plasma data. **FBP** contributed to data management and to the development of analysis scripts for MRI/PET analyses. **LD** contributed to MRI data acquisition and provided imaging research support. **BH** supervised the work. All authors critically revised the manuscript, provided feedback on previous versions, and approved the final version.

**Funding** Y.S. is a FRIA grantee of the Fonds de la Recherche Scientifique – FNRS (FRIA40014635). L.H. is a research fellow of the Fonds de la Recherche Scientifique – FNRS (FNRS40016560). V.M. was funded by Wallonia-Brussels International (WBI World Fellowship). FBP was funded by Innoviris Translate-AD. L.Q. is a postdoctoral research fellow of the Fonds de la Recherche Scientifique – FNRS (FC 95854). B.H. was funded by the FNRS, grant number CCL40010417, the FRFS-WELBIO, grant number 40010035, and Fondation Recherche Alzheimer/Stichting Alzheimer Onderzoek, grant numbers SAO20210026 and SAO20240044. Plasma analyses were funded by the MedReSyst-AI4Alzheimer project, which was supported by the European Union and Wallonia as part of the "Wallonia 2021-2027" program. We also thank the Fondation Louvain and the Saint-Luc Foundation for providing in-kind contributions.

**Data availability** The datasets used and analysed during the current study are available upon on reasonable request to Bernard.hanseeuw@uclouvain.be

## Declarations

**Ethics approval and consent to participate** Ethical approval for the study was granted by the UCLouvain Ethics Committee (13 May 2019; Eudra-CT number 2018-0034/73-94). Each participant provided informed consent.

**Competing interests** The authors declare no competing interests.



## References

1. Hyman BT, Phelps CH, Beach TG, et al. National Institute on Aging–Alzheimer's Association guidelines for the neuropathologic assessment of Alzheimer's disease. Alzheimers Dement. 2012;8:1–13.
2. Ossenkoppele R, Cohn-Sheehy BI, La Joie R, et al. Atrophy patterns in early clinical stages across distinct phenotypes of Alzheimer's disease. Hum Brain Mapp. 2015;36:4421–37.
3. Bejanin A, Schonhaut DR, La Joie R, et al. Tau pathology and neurodegeneration contribute to cognitive impairment in Alzheimer's disease. Brain. 2017;140:3286–300.
4. Hanseeuw BJ, Betensky RA, Jacobs HIL, et al. Association of amyloid and tau with cognition in preclinical Alzheimer disease: a longitudinal study. JAMA Neurol. 2019;76:915.
5. Wuestefeld A, Xie L, McGrew E, et al. Tau, atrophy, and domain-specific cognitive impairment in typical Alzheimer's disease. Alzheimers Dement. 2025;21:e70511.
6. Braak H, Braak E. Neuropathological stageing of Alzheimer-related changes. Acta Neuropathol (Berl). 1991;82:239–59.
7. Braak H, Braak E. Argyrophilic grain disease: frequency of occurrence in different age categories and neuropathological diagnostic criteria. J Neural Transm. 1998;105:801–19.
8. Xie L, Wisse LEM, Das SR, et al. Longitudinal atrophy in early Braak regions in preclinical Alzheimer's disease. Hum Brain Mapp. 2020;41:4704–17.
9. Chauveau L, Kuhn E, Palix C, et al. Medial temporal lobe subregional atrophy in aging and Alzheimer's disease: a longitudinal study. Front Aging Neurosci. 2021;13:750154.
10. Chen X, Toueg TN, Harrison TM, et al. Regional Tau deposition reflects different pathways of subsequent neurodegeneration and memory decline in cognitively normal older adults. Ann Neurol. 2024;95:249–59.
11. Wisse LEM, Xie L, Das SR, et al. Tau pathology mediates age effects on medial temporal lobe structure. Neurobiol Aging. 2022;109:135–44.
12. Xie L, Das SR, Wisse LEM, et al. Early tau burden correlates with higher rate of atrophy in transentorhinal cortex. J Alzheimers Dis. 2018;62:85–92.
13. Maass A, Berron D, Harrison TM, et al. Alzheimer's pathology targets distinct memory networks in the ageing brain. Brain. 2019;142:2492–509.

14. Stouffer KM, Grande X, Düzel E, et al. Amidst an amygdala renaissance in Alzheimer's disease. Brain. 2024;147:816–29.
15. Chen G, Xu T, Yan Y, et al. Amyloid beta: structure, biology and structure-based therapeutic development. Acta Pharmacol Sin. 2017;38:1205–35.
16. Lowe VJ, Wiste HJ, Senjem ML, et al. Widespread brain tau and its association with ageing, Braak stage and Alzheimer's dementia. Brain. 2018;141:271–87.
17. Schultz SA, Gordon BA, Mishra S, et al. Widespread distribution of tauopathy in preclinical Alzheimer's disease. Neurobiol Aging. 2018;72:177–85.
18 Insel PS, Mormino EC, Aisen PS, et al. Neuroanatomical spread of amyloid β and tau in Alzheimer's disease: implications for primary prevention. Brain Commun. 2020;2:fcaa007.
19. Yushkevich PA, Muñoz López M, Iñiguez De Onzoño Martin MM, et al. Three-dimensional mapping of neurofibrillary tangle burden in the human medial temporal lobe. Brain. 2021;144:2784–97.
20. Berron D, Vogel JW, Insel PS, et al. Early stages of tau pathology and its associations with functional connectivity, atrophy and memory. Brain. 2021;144:2771–83.
21. Stouffer KM, Chen C, Kulason S, et al. Early amygdala and ERC atrophy linked to 3D reconstruction of rostral neurofibrillary tau tangle pathology in Alzheimer's disease. NeuroImage Clin. 2023;38:103374.
22. Salman Y, Gérard T, Huyghe L, et al. Amygdala atrophies in specific subnuclei in preclinical Alzheimer's disease. Alzheimers Dement. 2024. https://doi.org/10.1002/alz.14235.
23. Baumeister H, Gellersen HM, Polk SE, et al. Disease stage–specific atrophy markers in Alzheimer's disease. Alzheimers Dement. 2025;21:e70482.
24. Brady DR, Mufson EJ. Amygdaloid pathology in Alzheimer's disease: qualitative and quantitative analysis. Dement Geriatr Cogn Disord. 1990;1:5–17.
25. Tsuchiya K, Kosaka K. Neuropathological study of the amygdala in presenile Alzheimer's disease. J Neurol Sci. 1990;100:165–73.
26. Price JL, McKeel DW, Buckles VD, et al. Neuropathology of nondemented aging: presumptive evidence for preclinical Alzheimer disease. Neurobiol Aging. 2009;30:1026–36.
27. Vogel JW, La Joie R, Grothe MJ, et al. A molecular gradient along the longitudinal axis of the human hippocampus informs large-scale behavioral systems. Nat Commun. 2020;11:960.
28. Saygin ZM, Kliemann D, Iglesias JE, et al. High-resolution magnetic resonance imaging reveals nuclei of the human amygdala: manual segmentation to automatic atlas. Neuroimage. 2017;155:370–82.
29. Tristão-Pereira C, Langella S, Sanchez JS, et al. Tau-PET pathology in the subregions of the amygdala and its associations with cognitive performance and neuropsychiatric symptoms in autosomal dominant Alzheimer's disease. Alzheimers Res Ther. 2025;17:64.
30. Mattsson-Carlgren N, Janelidze S, Palmqvist S, et al. Longitudinal plasma p-tau217 is increased in early stages of Alzheimer's disease. Brain. 2020;143:3234–41.
31. Colmant L, Boyer E, Gerard T, et al. Definition of a Threshold for the Plasma Aβ42/Aβ40 Ratio Measured by Single-Molecule Array to Predict the Amyloid Status of Individuals without Dementia. Int J Mol Sci. 2024;25:1173.
32. Karikari TK, Pascoal TA, Ashton NJ, et al. Blood phosphorylated tau 181 as a biomarker for Alzheimer's disease: a diagnostic performance and prediction modelling study using data from four prospective cohorts. Lancet Neurol. 2020;19:422–33.
33. Pereira JB, Janelidze S, Ossenkoppele R, et al. Untangling the association of amyloid-β and tau with synaptic and axonal loss in Alzheimer's disease. Brain. 2021;144:310–24.
34. Chong JR, Ashton NJ, Karikari TK, et al. Plasma P-tau181 to Aβ42 ratio is associated with brain amyloid burden and hippocampal atrophy in an Asian cohort of Alzheimer's disease patients with concomitant cerebrovascular disease. Alzheimers Dement. 2021;17:1649–62.
35. Cao J, Tang Y, Chen S, et al. The hippocampal subfield volume reduction and plasma biomarker changes in mild cognitive impairment and Alzheimer's disease. J Alzheimers Dis. 2024;98:907–23.
36. Rich A, Oh H. Alzheimer's Disease Neuroimaging Initiative. Distinctive associations between plasma p-tau181 levels and hippocampal subfield volume across the Alzheimer's disease continuum. Epub ahead of print 28 January 2025. https://doi.org/10.1101/2025.01.27.635113.
37. Horinek D, Petrovicky P, Hort J, et al. Amygdalar volume and psychiatric symptoms in Alzheimer's disease: an MRI analysis. Acta Neurol Scand. 2006;113:40–5.
38. Poulin SP, Dautoff R, Morris JC, et al. Amygdala atrophy is prominent in early Alzheimer's disease and relates to symptom severity. Psychiatry Res Neuroimaging. 2011;194:7–13.
39. Roh JH, Qiu A, Seo SW, et al. Volume reduction in subcortical regions according to severity of Alzheimer's disease. J Neurol. 2011;258:1013–20.
40. Benarroch EE. The amygdala: functional organization and involvement in neurologic disorders. Neurology. 2015;84:313–24.

41. Goerlich KS, Votinov M, Dicks E, et al. Neuroanatomical and neuropsychological markers of amnestic MCI: a three-year longitudinal study in individuals unaware of cognitive decline. Front Aging Neurosci. 2017. https://doi.org/10.3389/fnagi.2017.00034.
42. Huyghe L, Gérard T, Colmant L, et al. Amygdala tau deposition best discriminates between stages of memory impairment. Alzheimers Dement. 2023;19:e083045.
43. Van der Linden M, Coyette F, Poitrenaud J, et al. L'épreuve de rappel libre / rappel indicé à 16 items (RL/RI-16). Solal; 2004. p. 25.
44. De Partz M-P, Bilocq V, De Wilde V. Lexis: tests pour le diagnostic des troubles lexicaux chez le patient aphasique. Louvain-la-Neuve [Belgique]: De Boeck Solal; 2012.
45. Morris JC, Heyman A, Mohs RC, et al. The Consortium to Establish a Registry for Alzheimer's Disease (CERAD). Part I. Clinical and neuropsychological assesment of Alzheimer's disease. Neurology. 1989;39:1159.
46. Rouleau I, Salmon DP, Butters N, et al. Quantitative and qualitative analyses of clock drawings in Alzheimer's and Huntington's disease. Brain Cogn. 1992;18:70–87.
47. Ivanoiu A, Dricot L, Gilis N, et al. Classification of non-demented patients attending a memory clinic using the new diagnostic criteria for Alzheimer's disease with disease-related biomarkers. J Alzheimers Dis. 2014;43:835–47.
48. Klunk WE, Koeppe RA, Price JC, et al. The Centiloid project: standardizing quantitative amyloid plaque estimation by PET. Alzheimers Dement. 2015;11:1.
49. Bayart J-L, Hanseeuw B, Ivanoiu A, et al. Analytical and clinical performances of the automated Lumipulse cerebrospinal fluid Aβ42 and T-Tau assays for Alzheimer's disease diagnosis. J Neurol. 2019;266:2304–11.
50. Gérard T, Colmant L, Malotaux V, et al. The spatial extent of tauopathy on [18F]MK-6240 tau PET shows stronger association with cognitive performances than the standard uptake value ratio in Alzheimer's disease. Eur J Nucl Med Mol Imaging. 2024. https://doi.org/10.1007/s00259-024-06603-2.
51. Crary JF, Trojanowski JQ, Schneider JA, et al. Primary age-related tauopathy (PART): a common pathology associated with human aging. Acta Neuropathol (Berl). 2014;128:755–66.
52. Gérard T, Colmant L, Malotaux V, et al. Tau PET imaging with [$^{18}$ F ] MK -6240: limited affinity for primary tauopathies and high specificity for Alzheimer's disease. Eur J Neurol. 2025;32:e70068.
53. Fischl B. Freesurfer. Neuroimage. 2012;62:774–81.
54. Heimer L, De Olmos JS, Alheid GF, et al. The human basal forebrain. Part II. In: Handbook of chemical neuroanatomy. Elsevier; 1999. p. 57–226.
55. Leuzy A, Binette AP, Janelidze S, et al. Detection of PART in vivo using tau-PET: preliminary findings using [$^{18}$ F] RO948. Alzheimers Dement. 2023;19:e079520.
56. Shinotoh H, Shimada H, Tagai K, et al. A tau PET study of primary age-related tauopathy in healthy volunteers: neuroimaging / normal brain aging. Alzheimers Dement. 2020;16:e041730.
57. Hayes AF. Beyond Baron and Kenny: statistical mediation analysis in the new millennium. Commun Monogr. 2009;76:408–20.
58. Jack CR, Petersen RC, Xu YC, et al. Medial temporal atrophy on MRI in normal aging and very mild Alzheimer's disease. Neurology. 1997;49:786–94.
59. Unger JW, Lapham LW, McNeill TH, et al. The amygdala in Alzheimer's disease: neuropathology and Alz 50 immunoreactivity. Neurobiol Aging. 1991;12:389–99.
60. Vogt LJK, Hyman BT, Van Hoesen GW, et al. Pathological alterations in the amygdala in Alzheimer's disease. Neuroscience. 1990;37:377–85.
61. Thal DR, Rüb U, Orantes M, et al. Phases of Aβ-deposition in the human brain and its relevance for the development of AD. Neurology. 2002;58:1791–800.
62. Nelson PT, Abner EL, Patel E, et al. The amygdala as a locus of pathologic misfolding in neurodegenerative diseases. J Neuropathol Exp Neurol. 2018;77:2–20.
63. Milà-Alomà M, Ashton NJ, Shekari M, et al. Plasma p-tau231 and p-tau217 as state markers of amyloid-β pathology in preclinical Alzheimer's disease. Nat Med. 2022. https://doi.org/10.1038/s41591-022-01925-w.
64. De Strooper B, Zetterberg H. Tracking the turning point in Alzheimer's disease. Science. 2026;392:468–9.
65. Thal DR, Poesen K, Vandenberghe R, et al. Alzheimer's disease neuropathology and its estimation with fluid and imaging biomarkers. Mol Neurodegener. 2025;20:33.
66. Roddy D, Kelly JR, Farrell C, et al. Amygdala substructure volumes in major depressive disorder. NeuroImage Clin. 2021;31:102781.
67. Peters KR, Rockwood K, Black SE, et al. Characterizing neuropsychiatric symptoms in subjects referred to dementia clinics. Neurology. 2006;66:523–8.
68. Pawlowski M, Meuth S, Duning T. Cerebrospinal fluid biomarkers in Alzheimer's disease—from brain starch to bench and bedside. Diagnostics (Basel). 2017;7:42.
69. Montoliu-Gaya L, Salvadó G, Therriault J, et al. Plasma tau biomarkers for biological staging of Alzheimer's disease. Nat Aging. 2025;5:2297–308.

70. Saygin ZM, Osher DE, Koldewyn K, et al. Structural connectivity of the developing human amygdala. PLoS One. 2015;10:e0125170.
71. Bocchetta M, Iglesias JE, Cash DM, et al. Amygdala subnuclei are differentially affected in the different genetic and pathological forms of frontotemporal dementia. Alzheimers Dement Diagn Assess Dis Monit. 2019;11:136–41.
72. Guarino A, Favieri F, Boncompagni I, et al. Executive functions in Alzheimer disease: a systematic review. Front Aging Neurosci. 2019;10:437.



## Authors and Affiliations

**Yasmine Salman[1,10] · Thomas Gérard[1,2] · Lara Huyghe[1] · Lise Colmant[1] · Vincent Malotaux[3] · Jean-Louis Bayart[1,4,5] · Emilien Boyer[1,6] · Flo Blondiaux Pirson[1] · Pascal Kienlen-Campard[6] · Laurence Dricot[1] · Renaud Lhommel[2] · Adrian Ivanoiu[7] · Lisa Quenon[1] · Bernard J. Hanseeuw[1,7,8,9]**

✉ Yasmine Salman
yasmine.salman@uclouvain.be

Thomas Gérard
thomas.gerard@uclouvain.be

Lara Huyghe
lara.huyghe@uclouvain.be

Lise Colmant
lise.colmant@uclouvain.be

Vincent Malotaux
vmmalota@bu.edu

Jean-Louis Bayart
Jean-Louis.BAYART@cspo.be

Emilien Boyer
emilien.boyer@uclouvain.be

Flo Blondiaux Pirson
flo.blondiaux@uclouvain.be

Pascal Kienlen-Campard
pascal.kienlen-campard@uclouvain.be

Laurence Dricot
laurence.dricot@uclouvain.be

Renaud Lhommel
renaud.lhommel@saintluc.uclouvain.be

Adrian Ivanoiu
adrian.ivanoiu@uclouvain.be

Lisa Quenon
lisa.quenon@uclouvain.be

Bernard J. Hanseeuw
Bernard.hanseeuw@uclouvain.be

[1] Louvain Aging Brain Lab, Institute of Neuroscience, UCLouvain, 53 Avenue Mounier, 1200 Brussels, Belgium

[2] Nuclear Medicine Department, Saint-Luc University Hospital, Avenue Hippocrate 10, 1200 Brussels, Belgium

[3] Department of Psychological & Brain Sciences, Boston University, Boston, MA 02215, USA

[4] Department of Laboratory Medicine, Clinique St-Pierre, Ottignies, Belgium

[5] Department of Laboratory Medicine, Cliniques Universitaires Saint-Luc, Bruxelles, Belgium

[6] Aging and Dementia Group, Institute of Neuroscience, UCLouvain, 53 Avenue Mounier, 1200 Brussels, Belgium

[7] Neurology Department, Saint-Luc University Hospital, Avenue Hippocrate 10, 1200 Brussels, Belgium

[8] WELBIO department, WEL Research Institute, Avenue Pasteur, 6, 1300 Wavre, Belgium

[9] Department of Radiology, Massachusetts General Hospital, Harvard Medical School, Boston, MA 02114-2696, USA

[10] Institute of Neuroscience, UCLouvain, Avenue Mounier 53/B1.53.05, 1200 Brussels, Belgium